



## Evaluating adsorptive potential of low-cost adsorbents and biopolymer composite for heavy metals removal

Ghulam Hussain, Iqra Jabbar\*, Muhammad Umar Farooq, Mehwish Anis, Muhammad Irfan Jalees

*Institute of Environmental Engineering and Research (IEER), University of Engineering & Technology (UET), Lahore, Pakistan, emails: iqra.jabbar96@gmail.com (I. Jabbar), ghussain@uet.edu.pk (G. Hussain), umarfarooq@uet.edu.pk (M.U. Farooq), mehwish@uet.edu.pk (M. Anis), jalees@uet.edu.pk (M.I. Jalees)*

Received 15 December 2021; Accepted 23 July 2022

---

### ABSTRACT

Removal of heavy metals from water is an essential requirement to avoid environmental impacts of these hazardous contaminants. In comparison to other techniques, adsorption is considered relatively low cost, sustainable and environmentally friendly. In this study adsorptive removal of three heavy metals: lead, copper and cadmium was evaluated using bio adsorbents: wheat straw ash (WSA), turf grass ash (TGA) and biopolymer composite (BPC). Minitab software, employing Box–Behnken method, was used for design of experiments and optimization of treatment parameters (pH, contact time, initial concentration, and adsorbent dose). Box–Behnken method gives suitable number of runs for adsorption process. Prepared adsorbents were characterized using Fourier-transform infrared spectroscopy (FTIR), scanning electron microscope (SEM) and X-ray diffraction (XRD) analysis. FTIR revealed the presence of carbonates and phosphates as major groups in ashes which have high tendency to react with metals. While SEM has shown ashes to be more porous than biopolymer composite. High porous structure enhances the removal efficiency. XRD analysis of ashes have shown silica presence while biopolymer composite has semi crystalline fiber and rhombohedral structure in it. Silica reacts with metals and help in removal. Ashes characterization reveals their high removal potential. Batch adsorption was carried out for the removal of three heavy metals. For lead, the removal efficiency was highest for WSA (93%) followed by BPC (91%) and TGA (87%). For copper the highest removal was obtained by TGA (i.e., 93%) followed by BPC (92%) and WSA (89%). Similarly, for cadmium highest removal of 90% was attained by TGA, while 90% and 84% by WSA and BPC respectively. Significant parameters for lead and cadmium removal were initial concentration and pH according to Pareto chart of standardize effects. For copper it was contact time and interaction of pH with adsorbent dose.

*Keywords:* Adsorption; Heavy metals; Turf grass; Wheat straw; Biopolymer composite

---

### 1. Introduction

Degradation of water resources because of industrial effluent discharges is a long-standing environmental concern due to release of heavy metals [1]. On releasing into environment these metals can result in the contamination of

water and soil [2,3]. These metals enter in the human body through food chain and then from toxic bio-stable compound by combining with enzymes, polymers, proteins and DNA molecules and results in their improper functioning [4]. Some metals like arsenic, cadmium and lead are highly toxic and have carcinogenic, mutagenic, and genotoxic effects.

---

\* Corresponding author.

Water treatment techniques are vital to remove different contaminants. Based on region and sources of water, distinct water treatment technologies are used. Such technologies, starting from simple to advanced, are designed to ensure low-cost and environmental friendly sanitation and at the same time as potential benefits for water reuse [5]. Among all the techniques, adsorption is considered to be one of the efficient, sustainable and economical technique and easy to operate for removal of pollutants from effluents [6]. Different materials like activated carbon, waste mud, agricultural bio-waste, silica gel have been used as adsorbent but some of these are costly and some have low efficiency. There is a need to adopt approaches that increase and compare new adsorbent substances for wastewater treatment [7].

The use of nanomaterials and biopolymer composites as adsorbents is getting prominence [8,9]. Conventional petrochemical-based polymers are usually resisted because of their production from non-renewable resources and their resistance to biodegradation. So, natural biopolymer composites are supposed to be the safe and sustainable resources in this regard [10]. Bhullar et al. [11] conducted a study to analyze the effect of biopolymer based composite hydrogel in removal of Rhodamine 6G dye. The study showed that up to 87% removal could be achieved by using chitosan-based biopolymer composite hydrogel. Malayoglu [12] studied the adsorption capacity of chitosan/nanoclay composite for the removal of Cu(II) and Ni(II). The adsorbent was synthesized by using surfactant clay and chitosan biopolymer under polymerization method. Good removal efficiencies were achieved by using this adsorbent [12].

This study is aimed at evaluating some new, low cost, and environmentally friendly adsorbents to treat metals from aqueous solutions. Design of experiment has been employed for optimizing the adsorption conditions, which has rarely been used for the adsorption process in past studies. The study involves the use of wheat straw ash, turf grass ash and biopolymer composite derived from turf grass as adsorbents for removal of lead, nickel, and chromium from aqueous solutions. Several studies have been conducted on determining the adsorption capacities of wheat straw and its modifications, [13] the use of wheat straw ash, turf grass, and turf grass ash as adsorbent has not yet been explored. Further, biopolymer composite prepared from turf grass ash is also explored as novel adsorbent in this study.

## 2. Experimental

### 2.1. Materials

Wheat straw and turf grass was obtained from local fields and parks. Analytical grade chemicals including copper sulfate, cadmium chloride, lead nitrate, starch solution, HCl, ammonium per disulfate and methanol, were purchased from Sigma-Aldrich, USA used. All chemical solutions were freshly prepared for each experimentation.

### 2.2. Adsorbents preparation

Wheat straw and turf grass was washed with tap water several times to remove dust, dried and then burnt under

controlled conditions at 575°C for 8 h in an electrical furnace (MHA-11 OGAWA SEIKI). The ashes obtained were stored in a glass container and named as wheat straw ash (WSA) and turf grass ash (TGA). Starch composite turf grass was prepared by dissolving 6% starch solution in 50 mL water and stirring it for 15 min. This mixture was kept in ice bath and 250 mL of ammonium per disulfate was added in 50 mL HCl dropwise and 1 g of turf grass was added. Prepared mixture was stirred for 30 min. It was then placed at room temperature until its color changed to dark green. The mixture was filtered and filter paper residue was washed with tap water and methanol. Finally, the prepared mass was dried at 50°C for 48 h in an oven [14]. The prepared material was stored in container and named as biopolymer composite (BPC).

### 2.3. Characterization of adsorbents

Scanning electron microscope (SEM; JEOL Japan) was used to determine the morphology of the adsorbents with 5.0 KX magnification and size of 5 mm. All samples were in powdered form. Fourier-transform infrared spectrophotometer (FTIR) (Agilent Cary 630 FTIR) was used for determining the functional groups present in the adsorbents. Additionally, wide angle X-ray diffraction (XRD) of wheat straw ash, turf grass ash and biopolymer composite were recorded using X-ray diffractometer (Benchtop D2 Phaser).

### 2.4. Design of experiments

Statistically optimizing the parameters that affect the adsorption process is crucial to adsorption studies [15]. Hence, design of experiments and statistical optimization of treatment variables was performed using Minitab software and Box–Behnken method. Parameters such as pH, initial concentration, contact time and adsorbent dose were taken as independent variables and the removal efficiency was taken as output [16]. Twenty-seven (27) runs per metal per adsorbent were obtained, making a total of 243 combinations. The factors and levels used in experimental design are presented in Table 1.

### 2.5. Batch adsorption experiments

Standard stock solutions for the metals were prepared, which were diluted to obtain required concentrations of 10, 20, 30, 40 and 50 ppm. For batch experiments, 100 mL sample of metal solution was taken in a flask, and after adjusting the pH, the adsorbent dose was added and stirred with magnetic shaker for selected contact time. The initial concentration, adsorbent dose, pH, and contact time were set as determined through design of experiments. After treatment, the samples were filtered and analyzed by atomic absorption spectrophotometer (PerkinElmer A-Analyst 800). Blank samples were also run for each set of experiments. Removal of heavy metals by different adsorbents at various factor combinations was determined by taking final concentration and concentration of blanks as reference [17].

Table 1  
Factors and their levels used for experimental design

Factor	Coded symbol	Low level (-1)	High level (+1)
Contact time (min)	A	20	60
pH	B	3	8
Initial concentration (mg/L)	C	10	50
Adsorbent dosage (g/L)	D	0.05	0.25

### 3. Results and discussions

#### 3.1. Functional groups in prepared adsorbents

The FTIR spectra of turf grass biopolymer composite (Fig. 1a) showed peaks at 3,350; 1,653; 1,640 and 1,172  $\text{cm}^{-1}$ . Similar peaks have been identified in biopolymer composites in earlier studies [18]. The broad peak at 3,350  $\text{cm}^{-1}$  is due to asymmetric stretching vibration of  $-\text{OH}$  functional group [19–21], peak at 1,653  $\text{cm}^{-1}$  is attributed to  $-\text{C}=\text{C}$  alkene stretch, peak at 1,640  $\text{cm}^{-1}$  is attributed to aromatic skeletal stretching [19], and peak at 1,172  $\text{cm}^{-1}$  is due to  $\text{C}-\text{O}$  ester stretch [22]. FTIR spectra of wheat straw ash (Fig. 1b) showed comparable peaks with literature reported values at 1,677; 1,595; 1,461; 1,267; 1,110; 1,110.7; 1,066; 998 and 864  $\text{cm}^{-1}$  [23]. The peak at 1,677 and 1,595  $\text{cm}^{-1}$  represents carbonates. Peak at 1,461  $\text{cm}^{-1}$  is due to  $\text{C}=\text{N}$  stretch, whereas other lower peaks are due to  $\text{P}-\text{O}$  bond in  $\text{PO}_4^{3-}$  and siloxane ( $\text{Si}-\text{O}-\text{Si}$ ) [24]. FTIR analysis

of turf grass ash (Fig. 1c) showed peaks at 1,647; 1,416 and 892  $\text{cm}^{-1}$  similar to those found in wheat straw ash. Peaks at 1,647 and 1,416  $\text{cm}^{-1}$  are attributed to  $-\text{P}-\text{O}$  bond, while peak at 892  $\text{cm}^{-1}$  is attributed to  $\text{Si}-\text{O}-\text{Si}$  bond.

#### 3.2. Morphological analysis

SEM images for BPC, WSA and TGA are presented in Fig. 2. From the images it can be seen that that surface structure of these samples are porous which could allow metals to be absorbed on them [25]. Images of WSA (Fig. 2b) and TGA (Fig. 2c) have more porous structure than BPC (Fig. 2a). This could be the reason for increased removal efficiency of ashes than biopolymer composite.

#### 3.3. Crystalline structure of adsorbents

XRD analysis technique is used to determine the crystalline phases present in the substance and thereby

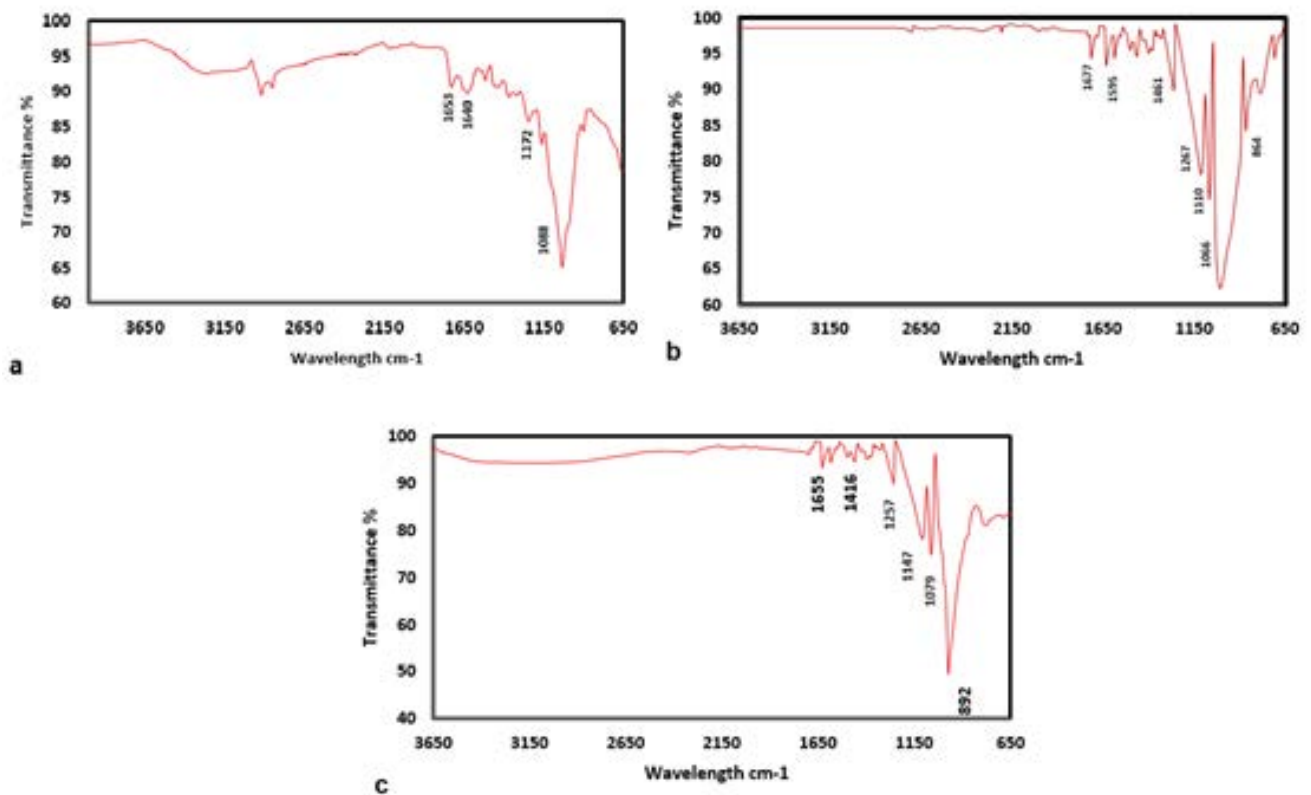


Fig. 1. FTIR spectra of (a) biopolymer composite, (b) wheat straw ash, and (c) turf grass ash.

helps in finding the chemical composition of the substance [26]. From  $2\theta$  value the crystalline structure present in substance is determined. Biopolymer composite showed  $2\theta$  value of 18.57 and 26.47 in Fig. 3a which indicates the presence of semi crystalline nature of fiber and rhombohedral structure respectively [27]. Wheat straw ash in Fig. 3b shows no other mixed crystalline phases than  $\text{SiO}_2$ . It showed a  $2\theta$  value of 21.86 which represents the presence of silica. Similarly, turf grass ash also shows  $2\theta$  at 21.78 in Fig. 3c representing the presence of

silica. Ashes basically are amorphous structure and contain two major phases crystallite and quartz [28].

#### 3.4. Removal of metals by biopolymer composite

Table 2 contains summary of results obtained from batch adsorption studies. Detailed results are provided as supplementary data (Table S1). Using biopolymer composite as adsorbent, maximum removal efficiency achieved for lead, cadmium and copper was 93%, 91% and 90%, respectively.

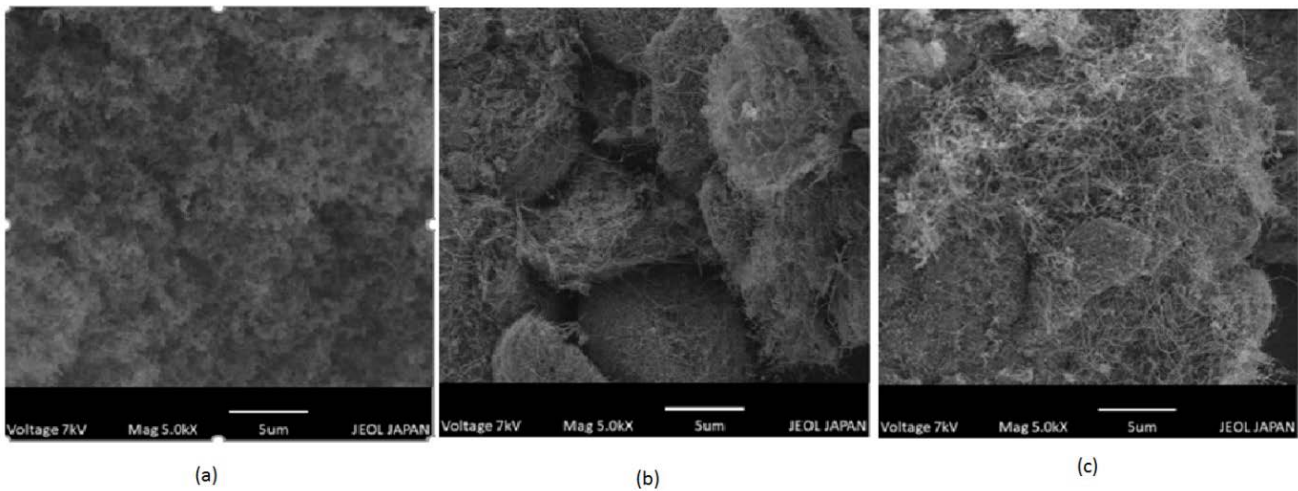


Fig. 2. SEM analysis of (a) biopolymer composite, (b) wheat straw ash, and (c) turf grass ash.

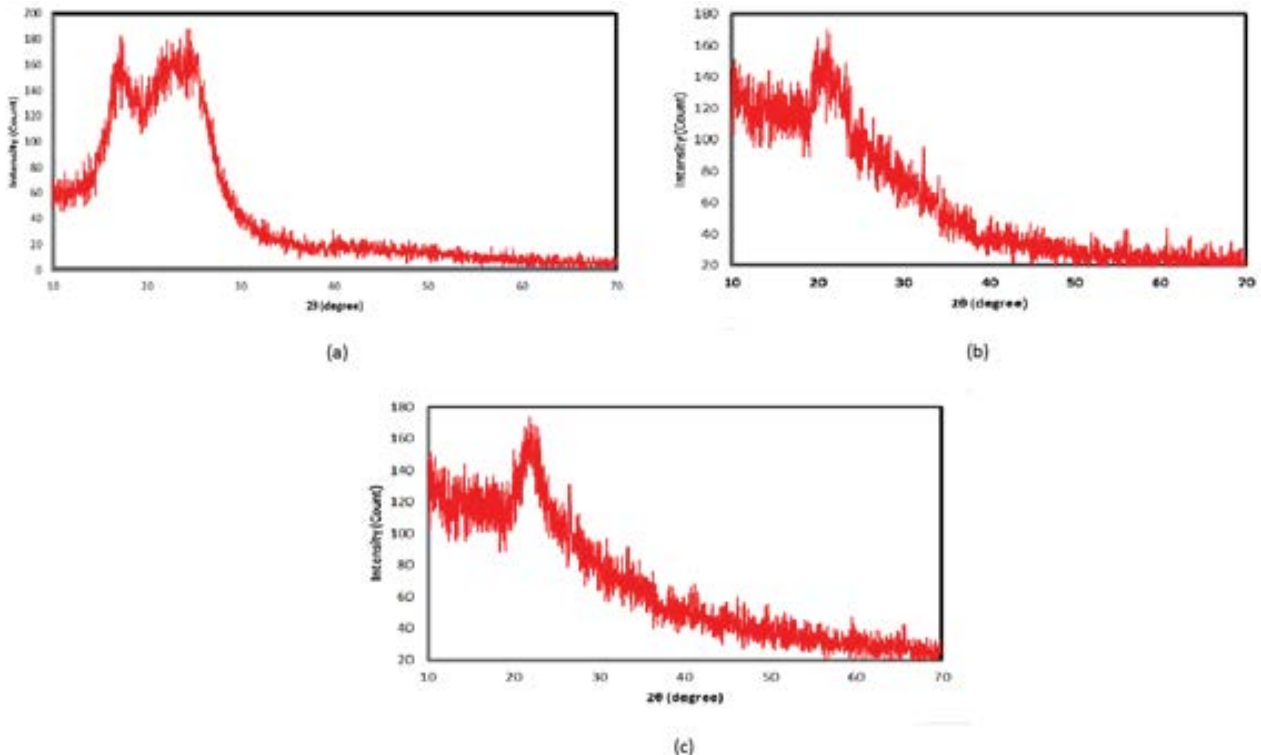


Fig. 3. XRD analysis of (a) biopolymer composite, (b) wheat straw ash, and (c) turf grass ash.

Table 2  
Summary of heavy metals removal efficiency by BPC

Metals	Removal efficiency (%)		
	Minimum	Mean	Maximum
Pb	84	89	93
Cd	56	77	81
Cu	85	87	90

The highest effectiveness for Pb and Cd was obtained at pH 5.5, contact time 40 min, initial concentration 30 mg/L and adsorbent dose of 0.25 g/L. For Cu, the maximum removal was at initial concentration of 10 mg/L.

Statistical analysis of all results was performed using analysis of variance (ANOVA) through Minitab 17. The results were obtained for a confidence level of 95%. It has revealed that linear and quadratic models were statistically significant with 95% confidence level. Pareto chart of standardized effects was used for evaluating the relative importance of the main effects and their interaction [29–33]. The graph depicts absolute values of effects from largest one to smallest one [34]. The bars demonstrate individual parameters and different possible combinations that can be obtained, while the x-axis represents values of student *t*-tests for each effect [30].

Pareto chart of standardized effects for adsorption of lead, cadmium, and copper on BPC are shown in Fig. 4. From Fig. 4a it can be seen that, of all the factors, initial concentration is more significant in removal process for lead removal. Whereas contact time has the least impact on removal efficiency. From Fig. 4b it can be seen that pH and initial concentration are statistically significant parameters, hence play major role in removal process in case of cadmium. For copper removal, pH has highest influence on removal, however, there is no statistically significant parameter (Fig. 4c).

Fig. 5 represents the contour plots representing the impact of interaction of two parameters for metals removal by biopolymer composite, while taking remaining two parameters as fixed. Fig. 5a shows effect of interaction of initial concentration and adsorbent dose for lead removal using BPC. Efficient removal of lead was achieved in complete range of initial concentration and adsorbent dose. The effect of adsorbent dose is more significant in comparison to initial concentration. However, removal efficiency also increases with increase in initial concentration and highest removal is obtained for >25 mg/L initial concentration. Fig. 5b shows the impact of interaction of initial concentration and pH on removal efficiency of cadmium. It shows an increasing efficiency with increase in pH and initial concentration. Highest removal efficiency range (>80%) is obtained for pH 7–8 and initial concentration of 25–45 mg/L.

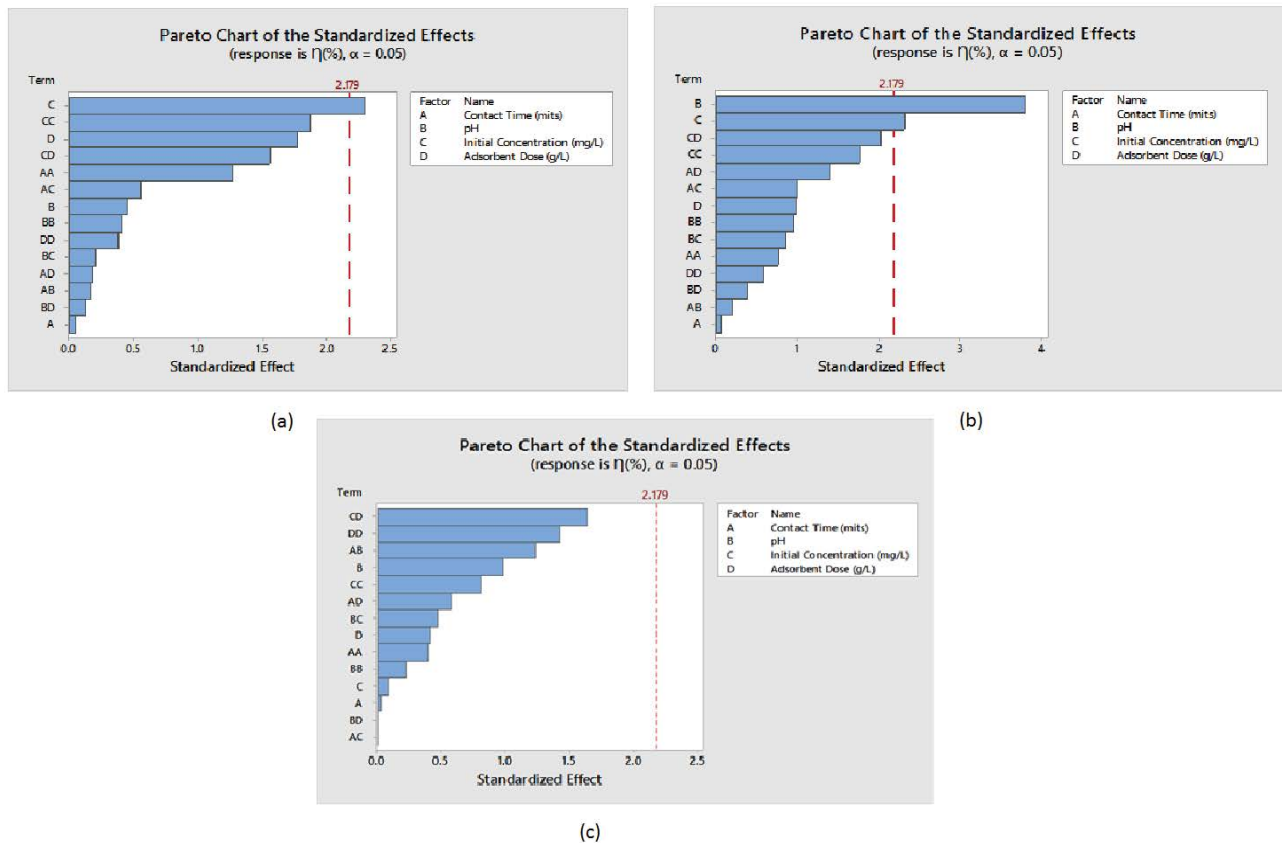


Fig. 4. Pareto chart of standardized effects for biopolymer composites (a) for lead, (b) for cadmium, and (c) for copper.

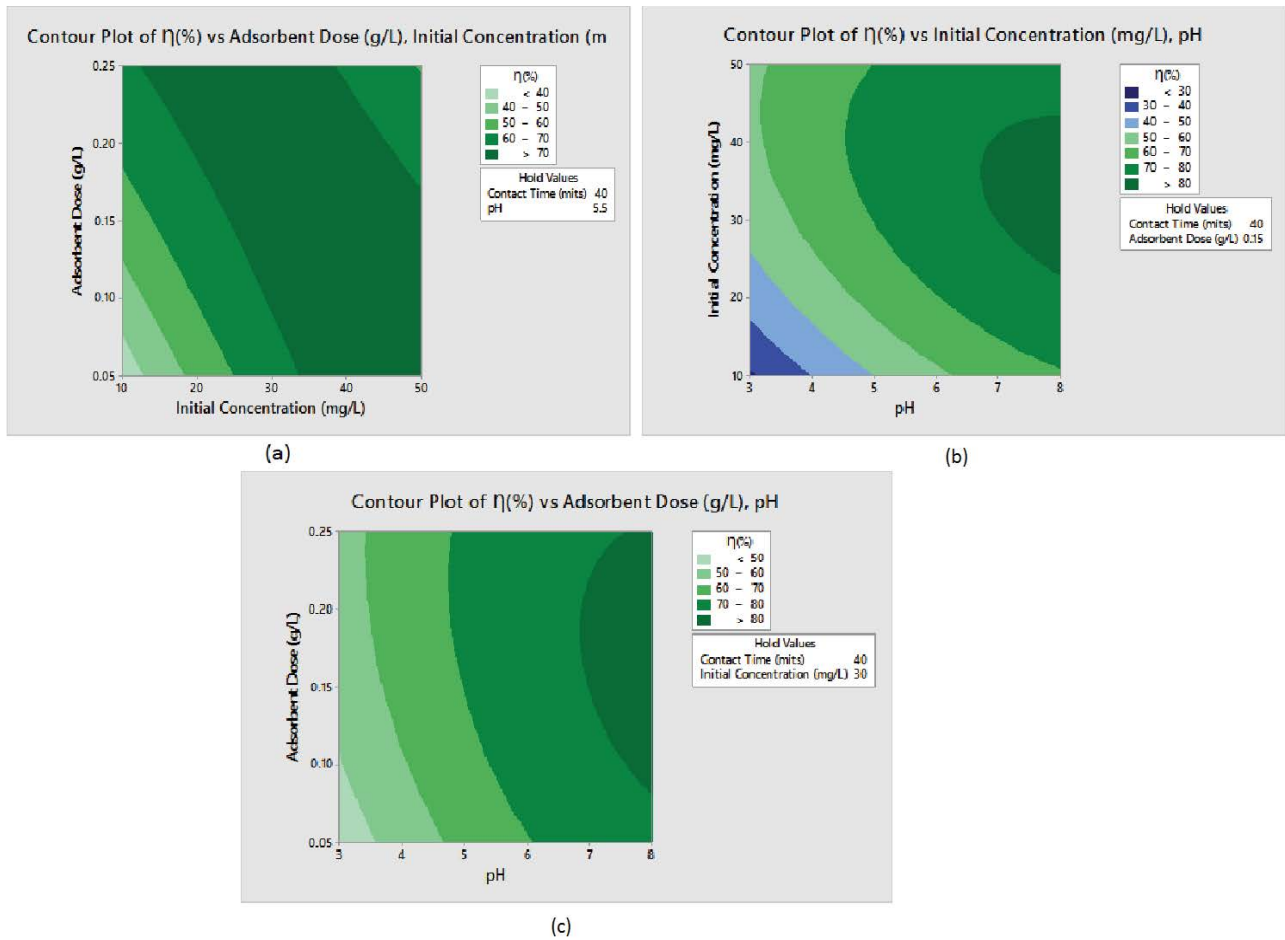


Fig. 5. Contour plots (a) for lead removal at contact time to be 40 min and pH to be 5.5, (b) for cadmium removal at contact time to be 40 min and adsorbent dose to be 0.15 g/L, and (c) for copper removal at contact time to be 40 min and initial concentration to be 30 mg/L.

For copper (Fig. 5c) removal, efficiency is increasing as pH is increasing, while adsorbent dose has less effect in combination to pH. Highest removal (>80%) was attained at pH 7–8 and a wide range of adsorbent doses (0.07–0.25 g/L).

### 3.5. Removal of metals by wheat straw ash

Table 3 presents the summarized results of metals removal using wheat straw ash as adsorbent. Detailed results are provided as supplementary data (Table S2). Maximum removal efficiency achieved for lead, cadmium and copper was 95%, 94% and 94%, respectively. The conditions that provided highest efficiencies are 5.5, contact time 40 min, initial concentration 30 mg/L, and adsorbent dose of 0.25 g/L. Minimum removal efficiency achieved for lead, cadmium and copper was 87%, 83% and 59%, respectively. Overall removal of lead and cadmium is better as compared to copper using WSA. Comparably, the removal of cadmium by WSA is better than BPC.

Pareto chart of standardized effects for adsorption of lead, cadmium, and copper on wheat straw ash are presented in Fig. 6. From Fig. 6a it can be seen that initial concentration is statistically more significant in removal process

Table 3  
Summary of heavy metals removal by wheat straw ash

Metals	Removal efficiency		
	Minimum	Maximum	Average
Pb	87	95	90
Cd	83	94	85
Cu	59	94	84

than other variables for lead removal. Whereas contact time has the least impact on removal efficiency. For cadmium removal, pH has the highest influence followed by contact time (Fig. 6b). While the contact time is the only statistically significant parameter for copper removal. Contact time has the highest effect on adsorption followed by pH (Fig. 6c).

Contour plots representing interaction of two variables, keeping other two fixed, on treatment performance of wheat straw ash are shown in Fig. 7. For lead removal (Fig. 7a), initially an increase in efficiency is observed with an increase in initial concentration. Later, a gradual decrease is observed with increase in initial concentration



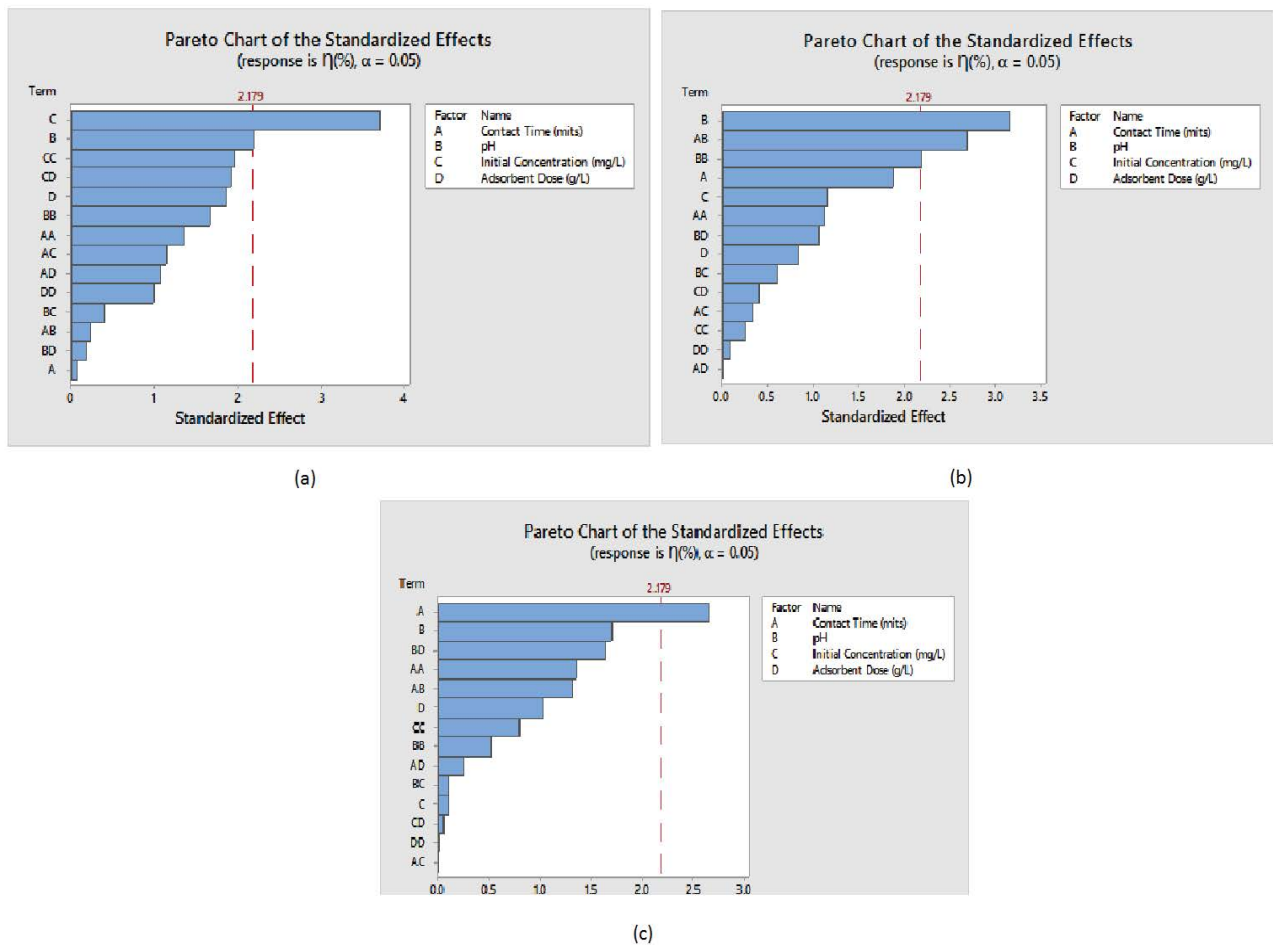


Fig. 6. Pareto chart of standardized effects for biopolymer composites (a) for lead, (b) for cadmium, and (c) for copper.

beyond 35 mg/L. While its removal increases with increase in adsorbent dose. Highest removal contour (>80%) was attained in combination of 0.23–0.25 g/L adsorbent dose and initial concentration of 25–35 mg/L. However, removal efficiency of lead increase with the increasing the adsorbent dosage. The contour for cadmium removal by wheat straw ash (Fig. 7b) showed an increase in removal efficiency with increase in contact time up to 30 min, where the maximum efficiency is achieved. Also, as pH increases, efficiency increases. The contour plot of copper removal by wheat straw ash (Fig. 7c) showed an increase in efficiency with increasing adsorbent dose but decrease in efficiency with increasing contact time. Higher dose means more active sites for metal to be adsorbed, while increasing contact time could cause logging of adsorbent resulting in less efficiency.

### 3.6. Removal of metals by turf grass ash

Summarized results of metals removal efficiency using turf grass ash as adsorbent are shown in Table 4. Detailed results are provided as supplementary data (Table S3). From Table 4, it can be found that maximum removal efficiency achieved for lead, cadmium and copper was 92%, 95% and 94%, respectively. The relevant conditions for

Table 4

Summary of heavy metals removal efficiency by turf grass ash

Metals	Removal efficiency		
	Minimum	Maximum	Average
Pb	67	92	87
Cd	87	95	79
Cu	84	94	88

highest lead removal were at pH 5.5, contact time 40 min, initial concentration 30 mg/L and adsorbent dose 0.25 g/L, for cadmium removal were pH 5.5, contact time 40 min, initial concentration 50 mg/L and adsorbent dose 0.25 g/L, while for copper were pH 5.5, contact time 40 min, initial concentration 30 mg/L and adsorbent dose 0.25 g/L. Minimum removal efficiency achieved for lead, cadmium and copper was 67%, 87% and 84%, respectively. Contrary to wheat straw ash and biopolymer composite, the removal efficiency of lead was quite low by turf grass ash. In addition, turf grass ash was very effective at removing copper as compared to other two adsorbents.

Pareto chart of standardized effects (Fig. 8) are presented for adsorption of lead, cadmium, and copper on

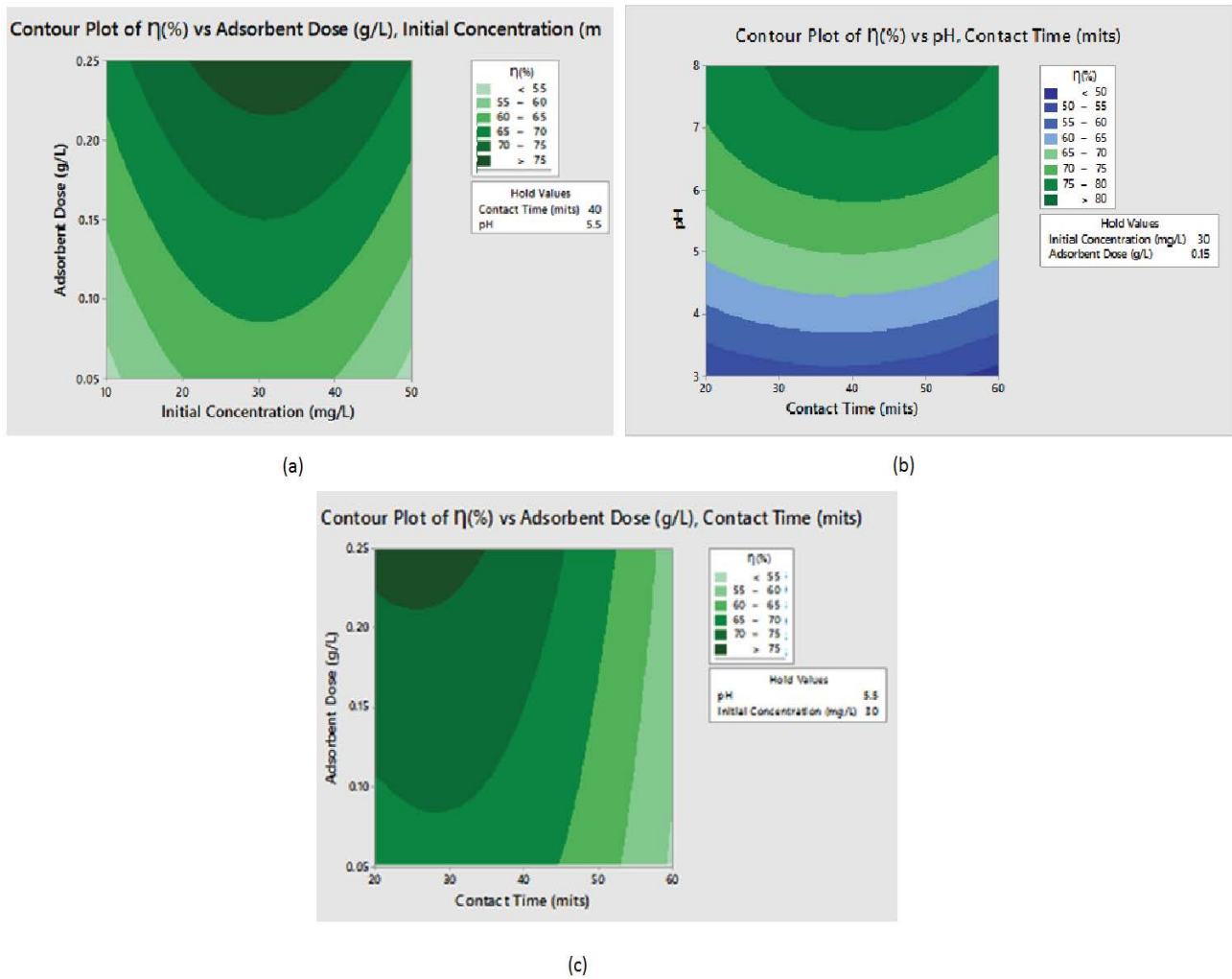


Fig. 7. Contour plots (a) for lead removal at contact time to be 40 min and pH to be 5.5, (b) for cadmium removal at contact time to be 40 min and adsorbent dose to be 0.15 g/L, and (c) for copper removal at pH to be 5.5 and initial concentration to be 30 mg/L.

Table 5  
R<sup>2</sup> values for adsorption isotherms for each metal and adsorbent

Adsorbent	Metal	R <sup>2</sup> values for adsorption isotherms			
		Langmuir	Freundlich	Temkin	Flory–Huggins
Biopolymer composite	Lead	0.92	0.92	0.91	0.93
	Cadmium	0.90	0.91	0.89	0.90
	Copper	0.91	0.92	0.89	0.93
Wheat straw ash	Lead	0.92	0.94	0.98	0.93
	Cadmium	0.94	0.94	0.93	0.93
	Copper	0.93	0.93	0.91	0.91
Turf grass ash	Lead	0.93	0.95	0.95	0.91
	Cadmium	0.92	0.97	0.97	0.92
	Copper	0.93	0.94	0.93	0.93

turf grass ash. From Fig. 8a it can be seen that initial concentration and interaction of pH with initial concentration is statistically more significant in removal process than other variables for lead. Whereas no parameter is

statistically significant in removal process for cadmium (Fig. 8b). For copper removal, the interaction of pH with adsorbent dose is the only statistically significant parameter (Fig. 8c).



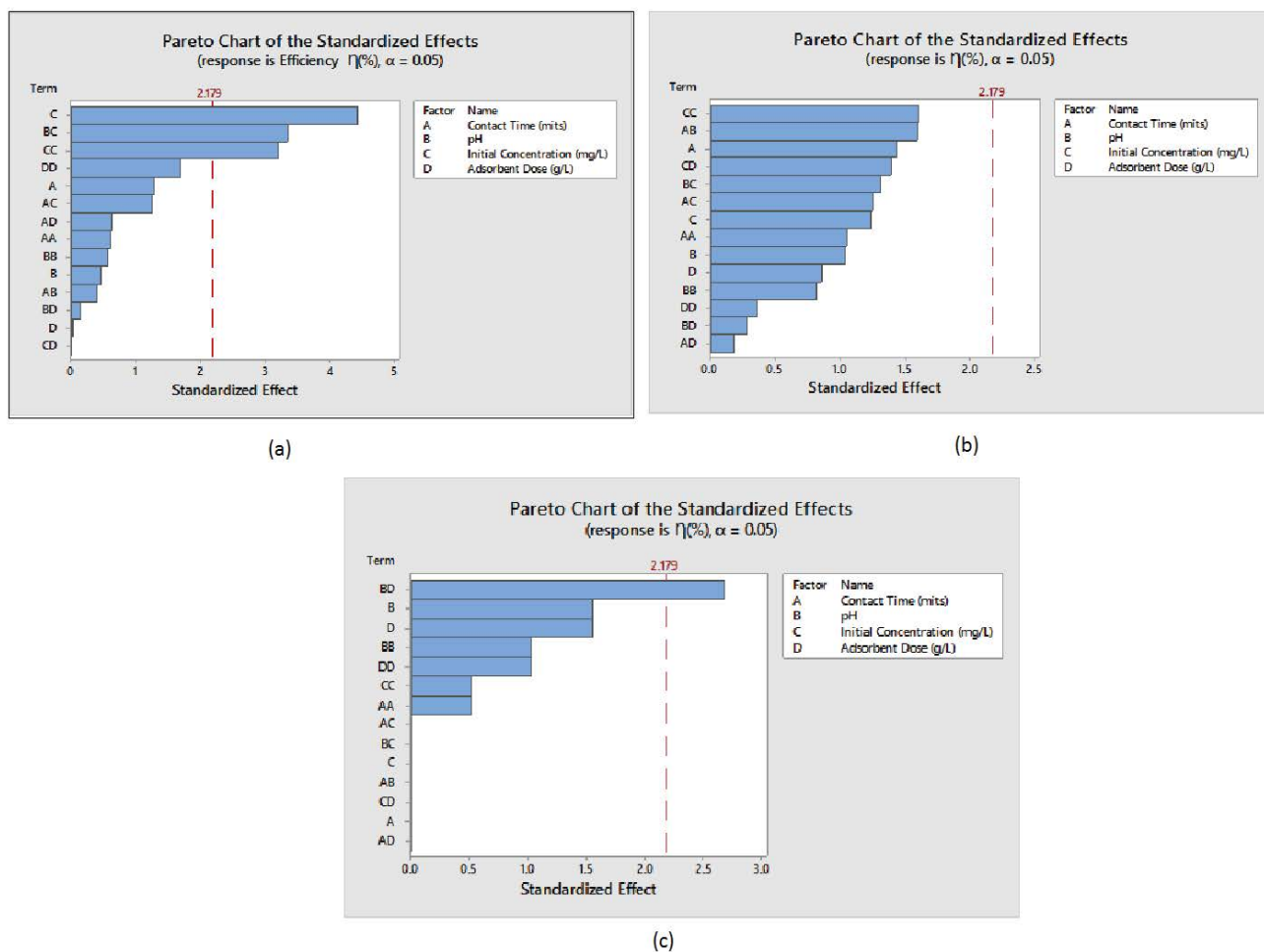


Fig. 8. Pareto chart of standardized effects for turf grass ash (a) for lead, (b) for cadmium, and (c) for copper.

Fig. 9 presents the contour plots describing the impact of interaction of variables on removal efficiency of lead by turf grass ash. For lead (Fig. 9a), as initial concentration of metal increases removal efficiency also increases because higher concentrations are easy to remove. The lead removal is good for all selected range of contact time. The contour in Fig. 9b represents the impact of interaction of pH and adsorbent dose at the removal of cadmium by turf grass ash, taking certain values of initial concentration at 30 mg/L and contact time at 40 min. It showed an increasing efficiency with increasing pH and increasing adsorbent dose. The contour diagram in Fig. 9c showed that increasing pH and adsorbent dose increases the removal efficiency of copper.

### 3.7. Study of isotherms

Adsorption isotherm study is important as it explain the relationship at equilibrium between the molecules of adsorbate and surface of the adsorbent. Thus, four different isotherm models were studied that expresses the surface characteristic and affinity of the adsorbent, that is, Langmuir, Freundlich, Temkin, and Flory–Huggins.

Table 5 shows the results of equilibrium data analysis for these models. Graphs of isotherm analysis for all metals and adsorbents are provided as supplementary data (Figs. S1–S9). Based on  $R^2$  value, it can be perceived that lead and copper removal by BPC followed Flory–Huggins isotherm, while cadmium removal is best fitted to Freundlich isotherm. Using WSA as adsorbent, lead removal followed Temkin isotherm, while cadmium and copper removal is best fitted to Langmuir isotherm. For TGA, lead and cadmium removal data was best fitted to Temkin isotherm, while copper removal followed Freundlich isotherm.

## 4. Conclusions

Adsorbents prepared from wheat straw and turf grass ashes contain functional groups of  $-P-O$  bond due to  $PO_4^{3-}$ , carbonates, and siloxane. Carbonates, siloxane, and phosphate react with the metals and enriches their removal. While biopolymer composite contains carbonyl group, aromatic esters, and  $P-O$  bonds. Besides, ashes have more porous structure as compared to biopolymer composite, hence better performance of ashes was observed for metals removal. The presence of crystalline structure of silica

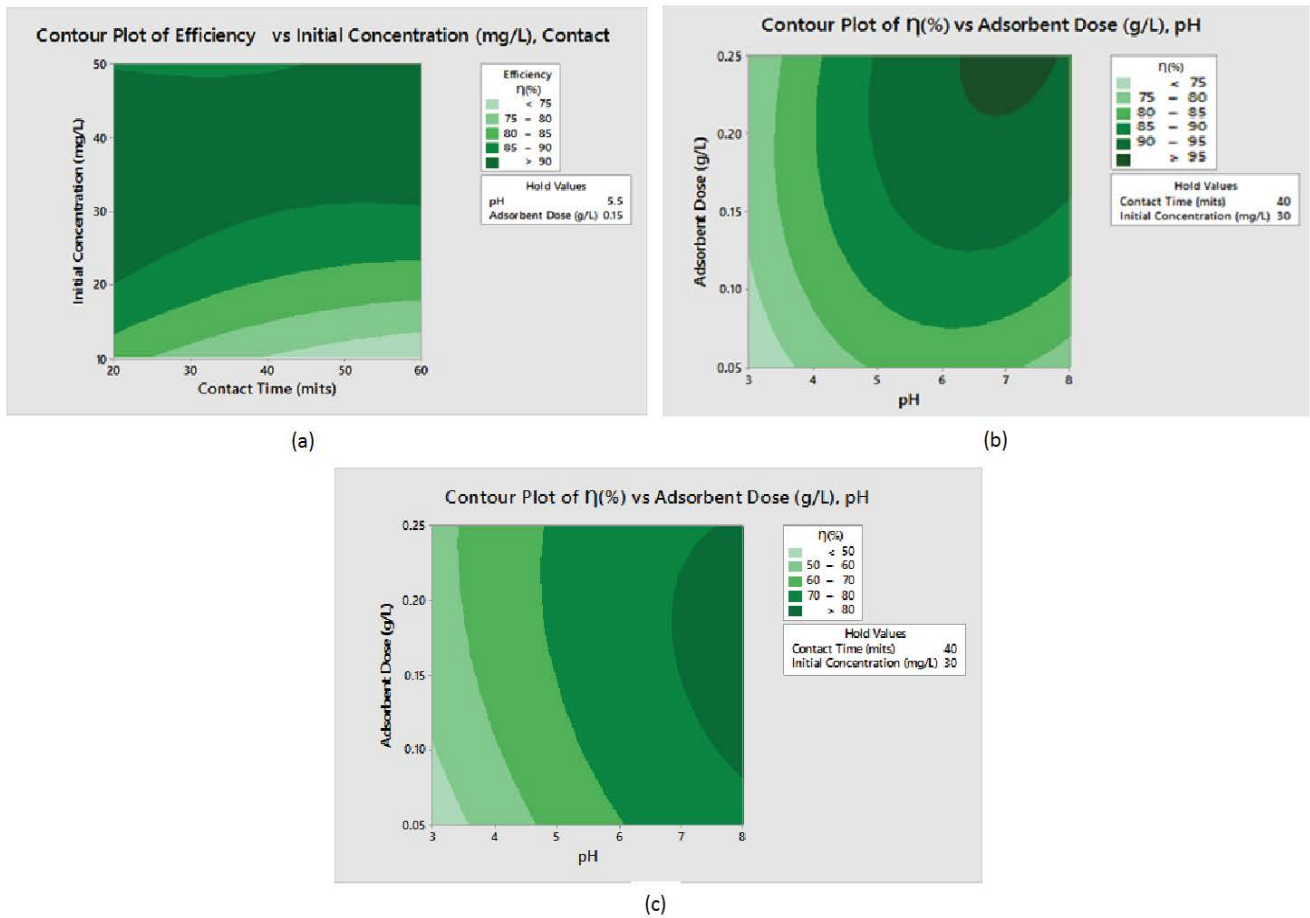


Fig. 9. Contour plots (a) for lead removal pH taken to be 5.5 and adsorbent dose to be 0.15 g/L, (b) for cadmium removal contact time taken to be 40 min and initial concentration to be 30 mg/L, and (c) for copper removal pH taken to be 5.5 and adsorbent dose to be 0.15 g/L, contact time taken to be 40 min and initial concentration to be 30 mg/L.

in ashes and crystalline structure of fiber and rhombohedral structure were found in biopolymer composite. Silica is found to be mainly responsible for removal of metals. For lead removal the efficiency of all adsorbents was in order of: WSA > BPC > TGA. For copper removal the efficiency of all adsorbents was in order of: TGA > BPC > WSA. For cadmium removal, the efficiency of all adsorbents was in order of: TGA > WSA > BPC. The studied adsorbents could be effectively employed for removal of heavy metals as cost effective and environmental friendly alternatives. For BPC, lead and copper removal followed Flory–Huggins isotherm, while cadmium removal was best fitted to Freundlich isotherm. Using WSA as adsorbent, lead removal followed Temkin isotherm, while cadmium and copper removal was best fitted to Langmuir isotherm. For TGA, lead and cadmium removal data was best fitted to Temkin isotherm, while copper removal followed Freundlich isotherm.

#### Statements and declarations

Ethical approval: Not applicable  
 Consent to participate: Not applicable  
 Consent to publish: Not applicable

#### Authors contributions

All authors contributed to the study conception and design. Material preparation, data collection and analysis were performed by Iqra Jabbar and Ghulam Hussain. The first draft of the manuscript was written by Iqra Jabbar, Ghulam Hussain, Muhammad Umar Farooq, Mehwish Anis and Muhammad Irfan Jalees. All authors reviewed and improved the manuscript.

#### Funding

The authors declare that no funds, grants, or other support were received during the preparation of this manuscript.

#### Competing interests

The authors have no relevant financial or non-financial interests to disclose.

#### Availability of data and materials

The authors confirm that the data supporting the findings of this study are available within the article and its supplementary materials.

## References

- [1] W.S. Chai, J.Y. Cheun, P. Senthil Kumar, M. Mubashir, Z. Majeed, F. Banat, S.-H. Ho, P.L. Show, A review on conventional and novel materials towards heavy metal adsorption in wastewater treatment application, *J. Cleaner Prod.*, 296 (2021) 126589, doi: 10.1016/j.jclepro.2021.126589.
- [2] A.A. Adeyemi, Z.O. Ojekunle, Concentrations and health risk assessment of industrial heavy metals pollution in groundwater in Ogun state, Nigeria, *Sci. Afr.*, 11 (2021) e00666, doi: 10.1016/j.sciaf.2020.e00666.
- [3] D. Paul, Research on heavy metal pollution of river Ganga: a review, *Ann. Agrar. Sci.*, 15 (2017) 278–286.
- [4] P. Lazor, J. Tomáš, T. Tóth, J. Tóth, S. Čéryová, Monitoring of air pollution and atmospheric deposition of heavy metals by analysis of honey, *J. Microbiol. Biotechnol. Food Sci.*, 1 (2012) 522–533.
- [5] T.A. Saleh, Trends in the sample preparation and analysis of nanomaterials as environmental contaminants, *Trends Environ. Anal. Chem.*, 28 (2020) e00101, doi: 10.1016/j.teac.2020.e00101.
- [6] H. Sadegh, G.A.M. Ali, Chapter 51 – Potential Applications of Nanomaterials in Wastewater Treatment: Nanoadsorbents Performance, In: *Research Anthology on Synthesis, Characterization, and Applications of Nanomaterials*, IGI Global, Hershey, PA, 2018, pp. 1230–1240.
- [7] T.A. Saleh, Protocols for synthesis of nanomaterials, polymers, and green materials as adsorbents for water treatment technologies, *Environ. Technol. Innovation*, 24 (2021) 101821, doi: 10.1016/j.eti.2021.101821.
- [8] A.T. Hoang, X.L. Bui, X.D. Pham, A novel investigation of oil and heavy metal adsorption capacity from as-fabricated adsorbent based on agricultural by-product and porous polymer, *Energy Sources Part A*, 40 (2018) 929–939.
- [9] T.A. Saleh, Nanomaterials: classification, properties, and environmental toxicities, *Environ. Technol. Innovation*, 20 (2020) 101067, doi: 10.1016/j.eti.2020.101067.
- [10] K. Palanisamy, A. Jeyaseelan, K. Murugesan, S.B. Palanisamy, *Biopolymer Technologies for Environmental Applications*, K. Gothandam, S. Ranjan, N. Dasgupta, E. Lichtfouse, Eds., *Nanoscience and Biotechnology for Environmental Applications. Environmental Chemistry for a Sustainable World*, Springer, Cham, 2019, pp. 55–83.
- [11] N. Bhullar, K. Kumari, D. Sud, A biopolymer-based composite hydrogel for rhodamine 6G dye removal: its synthesis, adsorption isotherms and kinetics, *Iran. Polym. J.*, 27 (2018) 527–535.
- [12] U. Malayoglu, Removal of heavy metals by biopolymer (chitosan)/nanoclay composites, *Sep. Sci. Technol.*, 53 (2018) 2741–2749.
- [13] A.B.D. Nandiyanto, R. Oktiani, R. Ragadhita, How to read and interpret FTIR spectroscopy of organic material, *Indones. J. Sci. Technol.*, 4 (2019) 97–118.
- [14] N. Tahir, H.N. Bhatti, M. Iqbal, S. Noreen, Biopolymers composites with peanut hull waste biomass and application for crystal violet adsorption, *Int. J. Biol. Macromol.*, 94 (2017) 210–220.
- [15] B. Maazinejad, O. Mohammadnia, G.A.M. Ali, A.S.H. Makhlof, M.N. Nadagouda, M. Sillanpää, A.M. Asiri, S. Agarwal, V.K. Gupta, H. Sadegh, Taguchi  $L_9(3^3)$  orthogonal array study based on methylene blue removal by single-walled carbon nanotubes-amine: adsorption optimization using the experimental design method, kinetics, equilibrium and thermodynamics, *J. Mol. Liq.*, 298 (2020) 112001, doi: 10.1016/j.molliq.2019.112001.
- [16] M.A. Khan, Momina, M.R. Siddiqui, M. Otero, S.A. Alshareef, M. Rafatullah, Removal of Rhodamine b from water using a solvent impregnated polymeric Dowex 5WX8 resin: statistical optimization and batch adsorption studies, *Polymers*, 12 (2020) 500, doi: 10.3390/polym12020500.
- [17] M. Sarstedt, J.F. Hair Jr, C. Nitzl, C.M. Ringle, M.C. Howard, Beyond a tandem analysis of SEM and PROCESS: use of PLS-SEM for mediation analyses, *Int. J. Market Res.*, 62 (2020) 288–299.
- [18] A. Munajad, C. Subroto, Suwarno, Fourier transform infrared (FTIR) spectroscopy analysis of transformer paper in mineral oil-paper composite insulation under accelerated thermal aging, *Energies*, 11 (2018) 364, doi: 10.3390/en11020364.
- [19] T.A. Saleh, Simultaneous adsorptive desulfurization of diesel fuel over bimetallic nanoparticles loaded on activated carbon, *J. Cleaner Prod.*, 172 (2018) 2123–2132.
- [20] T.A. Saleh, Isotherm, kinetic, and thermodynamic studies on Hg(II) adsorption from aqueous solution by silica-multiwall carbon nanotubes, *Environ. Sci. Pollut. Res.*, 22 (2015) 16721–16731.
- [21] T.A. Saleh, The influence of treatment temperature on the acidity of MWCNT oxidized by  $\text{HNO}_3$  or a mixture of  $\text{HNO}_3/\text{H}_2\text{SO}_4$ , *Appl. Surf. Sci.*, 257 (2011) 7746–7751.
- [22] A. Kendel, B. Zimmermann, Chemical analysis of pollen by FT-Raman and FTIR spectroscopies, *Front. Plant Sci.*, 11 (2020) 352, doi: 10.3389/fpls.2020.00352.
- [23] S. Praveenkumar, G. Sankarasubramanian, S. Sindhu, Strength, permeability and microstructure characterization of pulverized bagasse ash in cement mortars, *Constr. Build. Mater.*, 238 (2020) 117691, doi: 10.1016/j.conbuildmat.2019.117691.
- [24] A. Fareed, S.B.A. Zaidi, N. Ahmad, I. Hafeez, A. Ali, M.F. Ahmad, Use of agricultural waste ashes in asphalt binder and mixture: a sustainable solution to waste management, *Constr. Build. Mater.*, 259 (2020) 120575, doi: 10.1016/j.conbuildmat.2020.120575.
- [25] J.F. Hair Jr, M.C. Howard, C. Nitzl, Assessing measurement model quality in PLS-SEM using confirmatory composite analysis, *J. Bus. Res.*, 109 (2020) 101–110.
- [26] R.L. Moore, J.P. Mann, A. Montoya, B.S. Haynes, In situ synchrotron XRD analysis of the kinetics of spodumene phase transitions, *Phys. Chem. Chem. Phys.*, 20 (2018) 10753–10761.
- [27] P. Mohanty, S. Nanda, K.K. Pant, S. Naik, J.A. Kozinski, A.K. Dalai, Evaluation of the physicochemical development of biochars obtained from pyrolysis of wheat straw, timothy grass and pinewood: effects of heating rate, *J. Anal. Appl. Pyrolysis*, 104 (2013) 485–493.
- [28] D. Chen, X. Wang, X. Wang, K. Feng, J. Su, J. Dong, The mechanism of cadmium sorption by sulphur-modified wheat straw biochar and its application cadmium-contaminated soil, *Sci. Total Environ.*, 714 (2020) 136550, doi: 10.1016/j.scitotenv.2020.136550.
- [29] L. Wilkinson, Revising the Pareto chart, *Am. Stat.*, 60 (2006) 332–334.
- [30] T.A. Saleh, S.O. Adio, M. Asif, H. Dafalla, Statistical analysis of phenols adsorption on diethylenetriamine-modified activated carbon, *J. Cleaner Prod.*, 182 (2018) 960–968.
- [31] A. Sari, T.A. Saleh, M. Tuzen, Development and characterization of polymer-modified vermiculite composite as novel highly-efficient adsorbent for water treatment, *Surf. Interfaces*, 27 (2021) 101504, doi: 10.1016/j.surfin.2021.101504.
- [32] T.A. Saleh, A. Sari, M. Tuzen, Development and characterization of bentonite-gum Arabic composite as novel highly-efficient adsorbent to remove thorium ions from aqueous media, *Cellulose*, 28 (2021) 10321–10333.
- [33] T.A. Saleh, M. Tuzen, A. Sari, Evaluation of poly(ethylene diamine-trimesoyl chloride)-modified diatomite as efficient adsorbent for removal of rhodamine b from wastewater samples, *Environ. Sci. Pollut. Res.*, 28 (2021) 55655–55666.
- [34] N.D. Dejene, M. Gopal, The hybrid Pareto chart and FMEA methodology to reduce various defects in injection molding process, *Solid State Technol.*, 64 (2021) 3541–3555.

**Supplementary information**

Table S1  
Removal of heavy metals using biopolymer composite as adsorbent

Contact time (min)	pH	Initial concentration (mg/L)	Adsorbent dose (g/L)	Removal efficiency $\eta$ (%) for Pb	Efficiency $\eta$ (%) for Cd	Efficiency $\eta$ (%) for Cu
20	3	30	0.15	92	53	63
60	3	30	0.15	91	52	62
20	8	30	0.15	91	82	72
60	8	30	0.15	89	86	86
40	5.5	10	0.05	83	70	71
40	5.5	50	0.05	90	65	75
40	5.5	10	0.25	93	91	90
40	5.5	50	0.25	92	64	74
20	5.5	30	0.05	90	81	81
60	5.5	30	0.05	92	54	51
20	5.5	30	0.25	90	67	52
60	5.5	30	0.25	92	50	59
40	3	10	0.15	91	74	64
40	8	10	0.15	92	58	53
40	3	50	0.15	91	67	65
40	8	50	0.15	91	78	81
20	5.5	10	0.15	85	71	61
60	5.5	10	0.15	85	75	65
20	5.5	50	0.15	92	72	73
60	5.5	50	0.15	90	74	64
40	3	30	0.05	90	58	48
40	8	30	0.05	90	77	77
40	3	30	0.25	92	58	56
40	8	30	0.25	91	85	81
40	5.5	30	0.15	92	77	67
40	5.5	30	0.15	91	88	78
40	5.5	30	0.15	92	74	75

Table S2  
Removal of heavy metals using wheat straw ash as adsorbent

Contact time (min)	pH	Initial concentration (mg/L)	Adsorbent dose (g/L)	Removal efficiency $\eta$ (%) for Pb	Efficiency $\eta$ (%) for Cd	Efficiency $\eta$ (%) for Cu
20	3	30	0.15	90	92	93
60	3	30	0.15	90	91	93
20	8	30	0.15	92	92	93
60	8	30	0.15	91	93	66
40	5.5	10	0.05	87	91	89
40	5.5	50	0.05	92	89	88
40	5.5	10	0.25	92	86	93
40	5.5	50	0.25	93	92	93
20	5.5	30	0.05	91	91	93
60	5.5	30	0.05	90	92	93
20	5.5	30	0.25	91	90	93
60	5.5	30	0.25	92	90	88
40	3	10	0.15	89	87	92
40	8	10	0.15	89	87	90
40	3	50	0.15	92	91	93
40	8	50	0.15	91	91	93
20	5.5	10	0.15	89	93	93
60	5.5	10	0.15	91	92	61
20	5.5	50	0.15	93	90	93
60	5.5	50	0.15	92	85	62
40	3	30	0.05	90	87	93
40	8	30	0.05	93	92	59
40	3	30	0.25	90	91	92
40	5.5	30	0.25	95	94	94
40	5.5	30	0.15	92	92	93
40	5.5	30	0.15	92	85	93
40	5.5	30	0.15	93	83	93

Table S3  
Removal of heavy metals using turf grass ash as adsorbent

Contact time (min)	pH	Initial concentration (mg/L)	Adsorbent dose (g/L)	Efficiency $\eta$ (%) for Pb	Efficiency $\eta$ (%) for Cd	Efficiency $\eta$ (%) for Cu
20	3	30	0.15	90	94	93
60	3	30	0.15	88	87	92
20	8	30	0.15	85	93	92
60	8	30	0.15	87	93	90
40	5.5	10	0.05	75	89	84
40	5.5	50	0.05	90	94	91
40	5.5	10	0.25	72	93	93
40	5.5	50	0.25	87	95	93
20	5.5	30	0.05	91	93	91
60	5.5	30	0.05	85	93	93
40	5.5	30	0.25	92	93	91
60	5.5	30	0.25	91	94	94
40	3	10	0.15	84	91	92
40	8	10	0.15	67	93	93
40	3	50	0.15	69	94	92
40	8	50	0.15	91	93	92
20	5.5	10	0.15	74	93	86
60	5.5	10	0.15	59	94	86
20	5.5	50	0.15	91	94	93
60	5.5	50	0.15	91	91	91
40	3	30	0.05	90	94	91
40	8	30	0.05	88	94	91
40	3	30	0.25	91	93	93
40	8	30	0.25	90	94	92
40	5.5	30	0.15	80	94	93
40	5.5	30	0.15	80	94	92
40	5.5	30	0.15	92	94	93

Table S4  
Parameters of isotherms

	Langmuir	Freundlich
Equation	$Y = 3.88X + 41.14$	$Y = 0.48X + 3.28$
Intercept	$1/(K_L \times q_m) = 41.14$	$\ln K_F = 3.28$
Slope	$1/q_m = 3.88$ $q_m = 0.257$	$1/n = 0.48$ $n = 2.08$
Constant	$K_L = 0.094$	$K_F = 26.5$



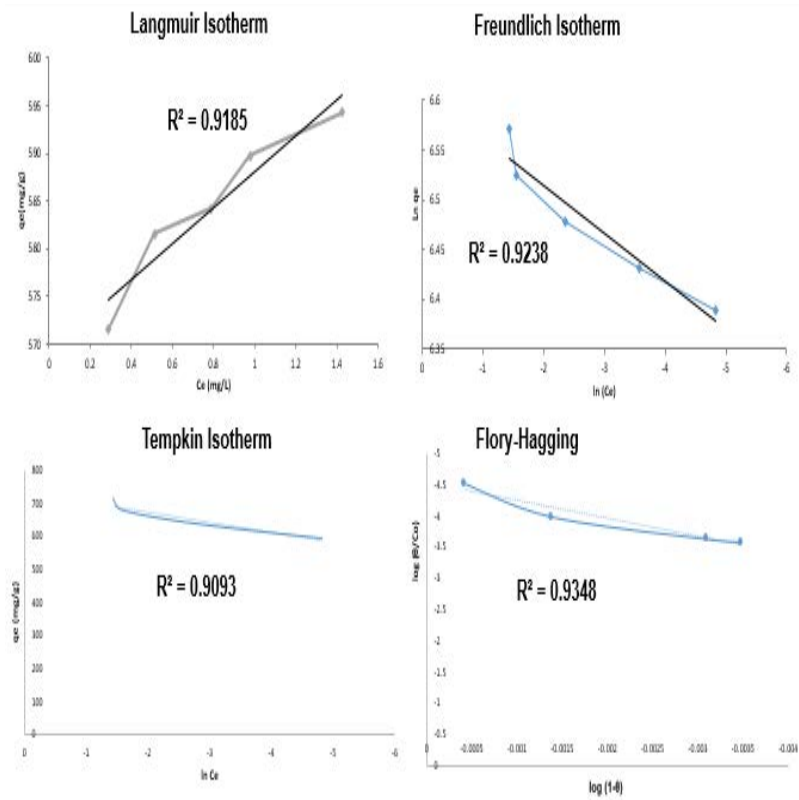


Fig. S1. Adsorption isotherm for lead using BPC.

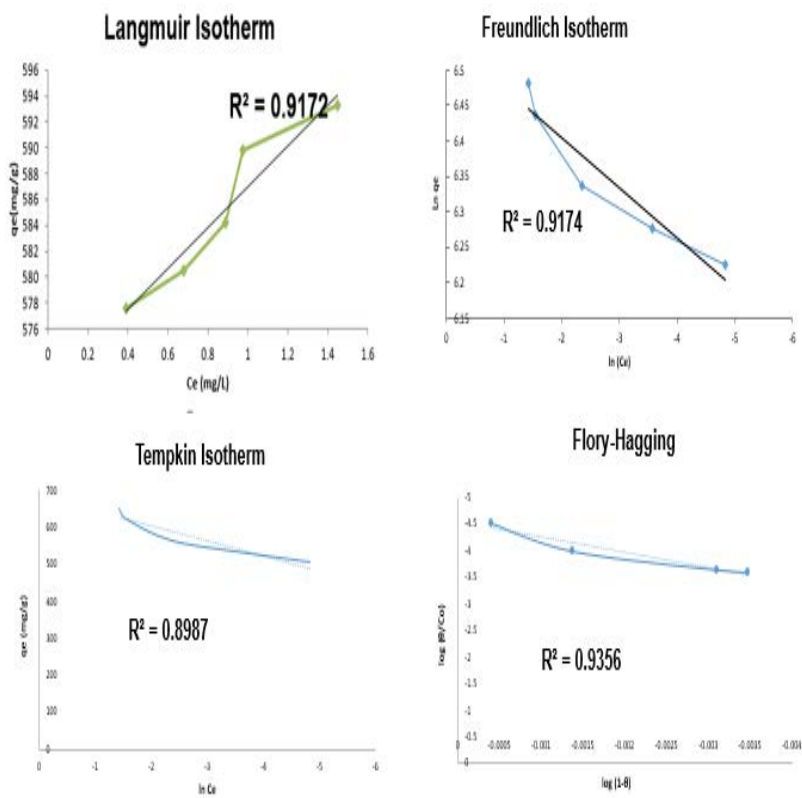


Fig. S2. Adsorption isotherms for copper using BPC.

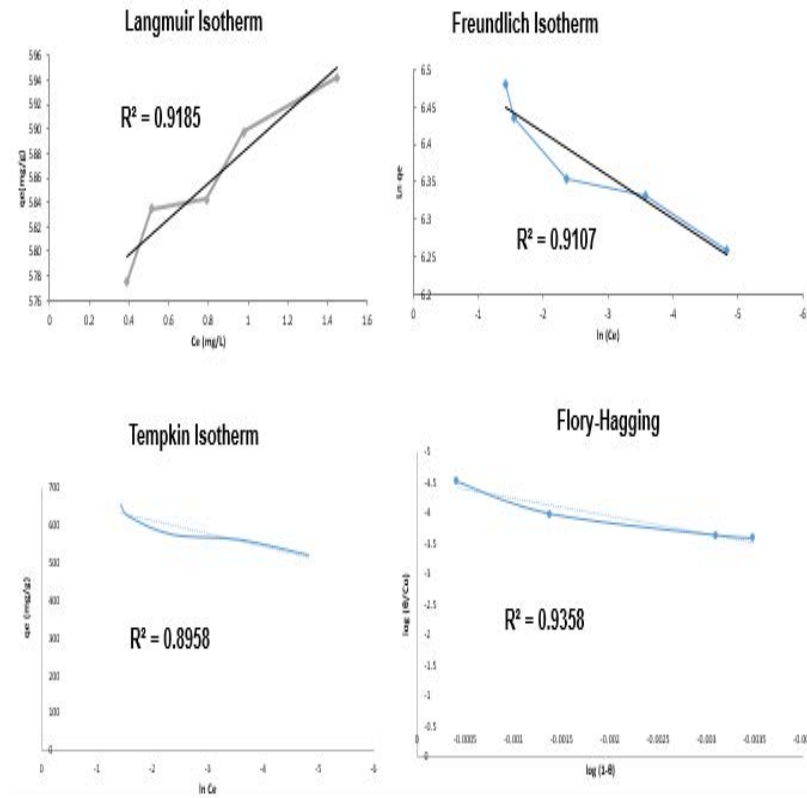


Fig. S3. Adsorption isotherms for cadmium using BPC.

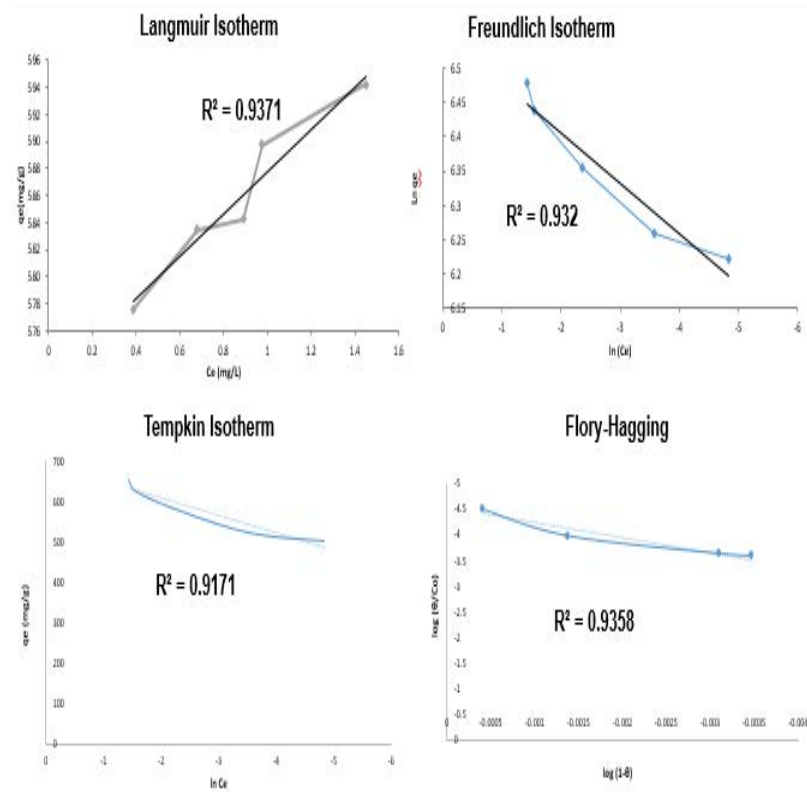


Fig. S4. Adsorption isotherm for copper using WSA.

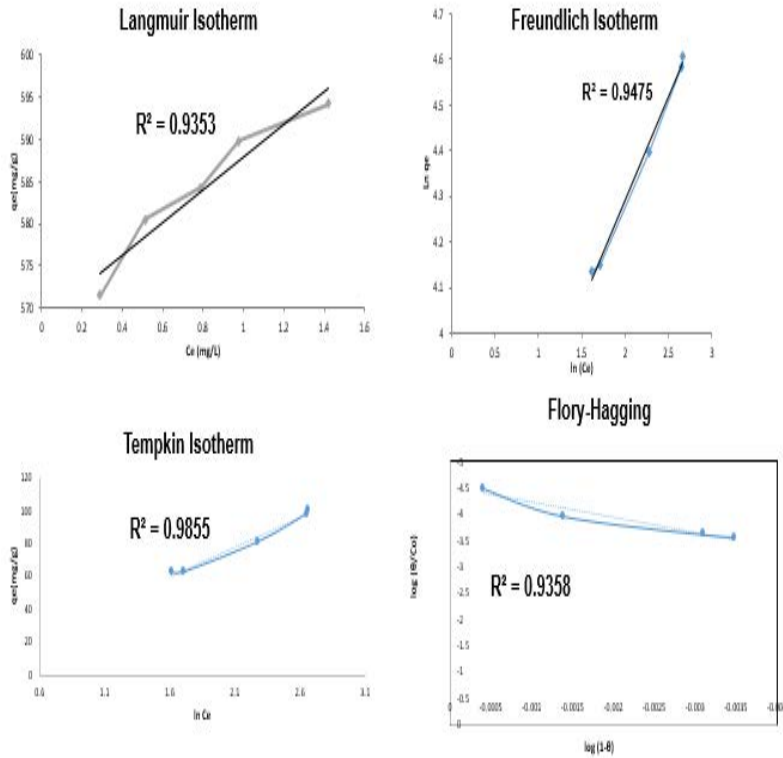


Fig. S5. Adsorption isotherm for lead using WSA.

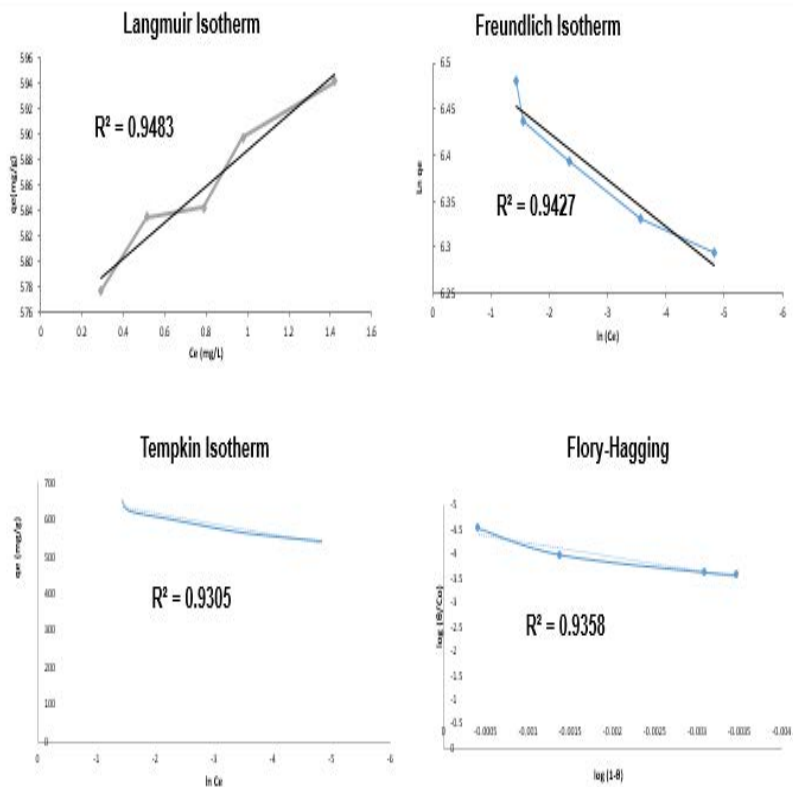


Fig. S6. Adsorption isotherms for cadmium using WSA.

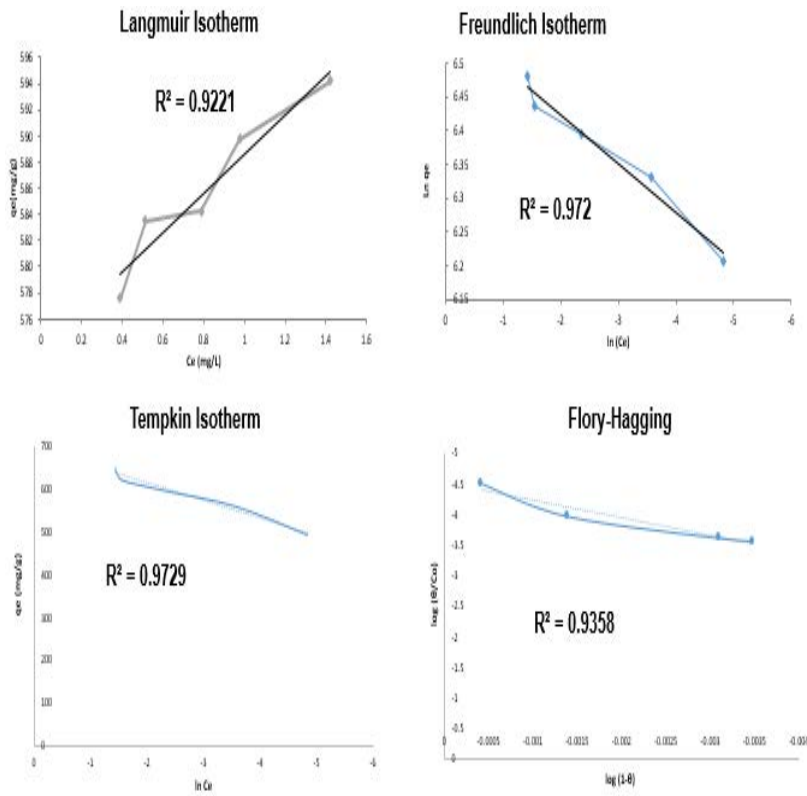


Fig. S7. Adsorption isotherms for cadmium using TGA.

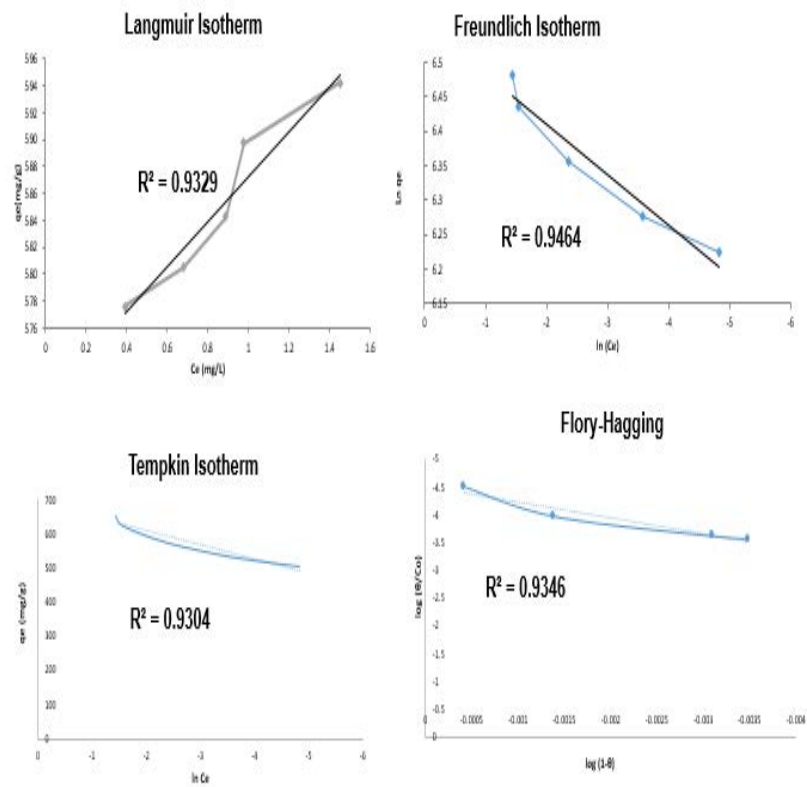


Fig. S8. Adsorption isotherms for copper using TGA.

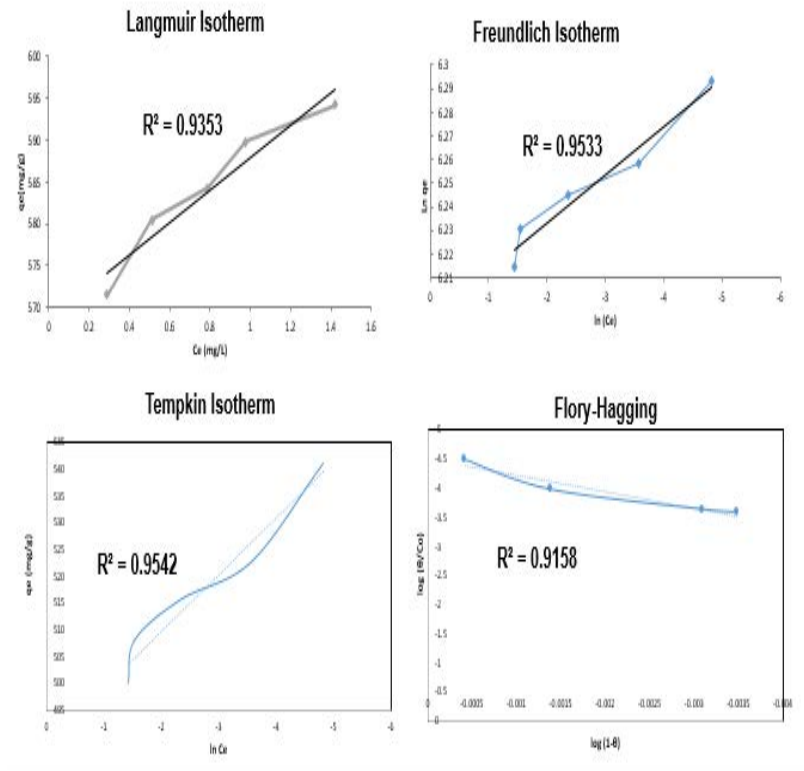


Fig. S9. Adsorption isotherms for lead using TGA.